# Electronic Supplementary Information

# Radar like Iron based Nanohybrid as Efficient and Stable Electrocatalyst for Oxygen Reduction

Xing Zhong,[a] Lin Liu,[a] Xinde Wang,[a] Huiyou Yu,[a] Guilin Zhuang,[a] Donghai Mei,[b] Xiaonian Li,[a] Jian-guo Wang*[a]

## *Contents*

# *1. General Experimental Section*

### *1.1 Materials*

Graphene Nanopowder (98%) were purchased from Graphene Supermarket (Graphene Laboratories Inc). Cesium fluoride (99%) and Acetonitrile (99.9%) were purchased from J&K Scientific Ltd. 20 wt% Pt/C were purchased from Alfa Aesar. Iron Phthalocyanine (95%) was purchased from J&K Scientific Ltd. Unless otherwise stated, all chemicals were used as received without further purification. De-ionized water (18.2 MΩ) was used throughout the experiments.

### *1.2 Instruments*

Transmission electron microscopy (TEM) images were performed on Tecnai G2F30S-Twin electron microscope operating at 300 kV. Atomic force microscopy (AFM) images were recorded with Tapping mode in a commercial Nanoscope VIII MultiMode SPM system (Bruker, Santa Barbara, CA).Thermogravimetric analysis (TGA) was measured under an argon atmosphere to 900 °C with a Perkin Elmer Thermal Analyzer at a heating rate of 10 °C min$^{-1}$. X-ray photoelectron spectroscopy (XPS) analysis was carried on Kratos AXIS Ultra DLD X-ray photoelectron spectrometer. Raman spectra were obtained by inVia Reinishaw confocal spectroscopy with 633nm laser excited.

Cyclic voltammetry (CV) experiments were performed on CHI660D Electrochemical analyzer (CHI Instrument Corp. Shanghai). Rotating disk electrode (RDE) measurements were performed on CHI 760C and MSR Electrode Rotator from Pine Research Instrumentation.

### *1.3 Materials synthesis*

Pyridyne precursors were prepared according to literature procedures.[1]

Pyridynes Cycloaddition of Graphene (PyNG)

Typically, 3,4-pyridyne precursor (5 mmol, 2.5 equiv. per graphene carbon) was added to an acetonitrile solution of the pristine graphene sheets (PG) (24 mg, 2mmol) and CsF (10 mmol, 5 equiv. per graphene carbon), the mixture was stirred at 80 ℃ for 24 h. After completion of the reaction, the 3,4-pyridyne cycloaddition of graphene (PyNG) were separated from the mixture by filtration, washed thoroughly with N,N-dimethylformamide (DMF), water and ethanol, in order to ensure that no residual pyridine and by-product remains, then collected and dried in vacuo.

Fe-PyNG

Typically, Fe-PyNG hybrid was prepared by heating the mixture of FePc (2.5 mg) and PyNG (5mg) in 20ml DMF under an Ar atmosphere at 60℃ for 3h. After completion of the reaction, the Fe-PyNG were separated from the mixture by filtration, washed thoroughly with DMF, water and ethanol, in order to ensure that no residual FePc remains, then collected and dried in vacuo. For the purpose of comparsion, in the similar way, the Fe-PG was also prepared by using FePc and PG.

### *1.4 Electrochemical characterization*

5 mg of the graphene samples were dispersed in a solution containing 4.8 ml of deionized water (18.2 MΩ) and 0.2 ml of 5 wt.% Nafion aqueous solution (1mg.ml$^{-1}$). The mixtures were ultrasonicated for 10 minutes to obtain a homogenous catalyst ink. To prepare the working electrode for electrochemical measurements, 10 µl of

the ink was dipped on a glass carbon electrode (4 mm in diameter). For comparison, a commercially available catalyst of 20 wt% Pt/C was used and 1 mg.ml$^{-1}$ suspension was also prepared as the same procedure described above, 5 μl of the 20 wt% Pt/C ink was dipped on a glass carbon electrode (4 mm in diameter). The electrode is allowed to dry at room temperature before measurement.

Cyclic voltammetry (CV) experiments：the working electrode was inserted into the cell setup, which is composed of a platinum counter electrode, an Ag/AgCl/KCl (3 M) reference electrode and a 30 ml glass cell containing 20 ml of 0.1 M KOH aqueous electrolyte. Before test, electrolyte was saturated with $O_2/N_2$ by bubbling $O_2/N_2$ prior to the start of each experiment. A flow of $O_2/N_2$ was maintained over the electrolyte during the recording of CVs in order to ensure its continued $O_2/N_2$ saturation. The potential range is cyclically scanned between -1.0 and +0.2 V at different scan rate of 100 mV s$^{-1}$ at the ambient temperature.

Rotating disk electrode (RDE) measurement: the same amount of catalyst was loaded on a rotating glass carbon electrode (3mm in diameter ). A Pt sheet and an Ag/AgCl/KCl (3 M) were used as the counter and reference electrodes, respectively. The linear sweep voltammograms of the modified glass carbon electrode were recorded in $O_2$ saturated 0.1 M KOH with a scan rate of 10 mV s$^{-1}$ at various rotating speeds from 400 to 2025 rpm. After each scan, the electrolyte was saturated with $O_2$ again for 20 minutes.

The Koutecky-Levich plots were obtained by linear fitting of the reciprocal rotating speed versus reciprocal current density collected at different potentials form -0.4 V to -0.8 V. The overall electron transfer numbers per oxygen molecule involved in a typical ORR process weere calculated from the slopes of Koutecky-Levich plots using the following equation:

$$\frac{1}{j} = \frac{1}{j_k} + \frac{1}{B\omega^{1/2}}$$

where j is the current, $j_k$ is the kinetic current, ω is the electrode rotating speed in rpm, and B is the Levich slope, which was determined from the slope of Koutecky-Levich plots based on Levich equation as followed:

$$B = 0.2nFC_0(D_0)^{2/3}v^{-1/6}$$

where n is the number of electrons transferred per oxygen molecule, F is the Faraday constant（96485 C mol$^{-1}$）, $D_0$ is the diffusion coefficient of $O_2$ in 0.1 M KOH ($1.9\times10^{-5}$ cm s$^{-1}$), $v$ is the kinetic viscosity, and $C_0$ is the concentration of $O_2$ ($1.2\times10^{-3}$ mol L$^{-1}$). The constant 0.2 is adopted when the rotating speed is in rpm.

## *2. Supplementary Results*

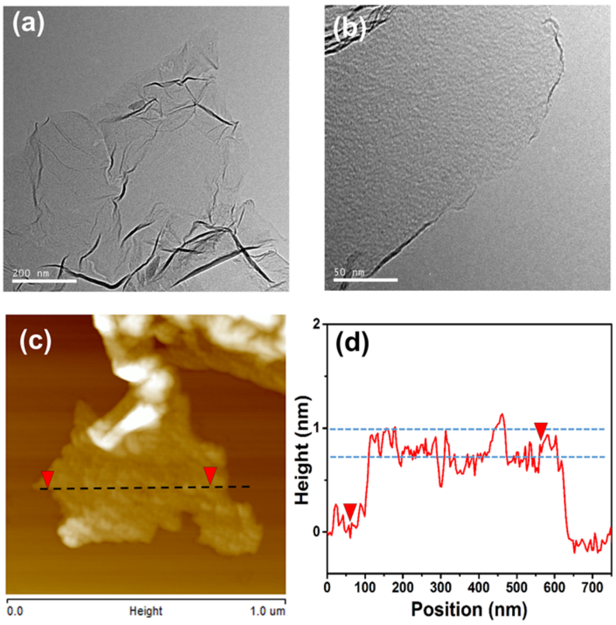

**Figure S1.** (a) TEM image of PG, Scale bar is 200 nm; (b) TEM image of PG, Scale bar is 50 nm; (c) Tapping mode AFM height image of PG and (d) corresponding height profile;

***Table S1:*** The calculated species concentrations (atomic %) of different atoms in PG, PyNG, Fe-PyNG and Fe-PG based XPS results.

| | **C** | **O** | **N** | **Fe** |
|---|---|---|---|---|
| **PG** | 96.97 | 2.68 | 0.35 | 0 |
| **PyNG** | 92.90 | 3.52 | 3.58 | 0 |
| **Fe-PyNG** | 91.88 | 3.61 | 4.20 | 0.31 |
| **Fe-PG** | 95.44 | 3.15 | 1.07 | 0.34 |

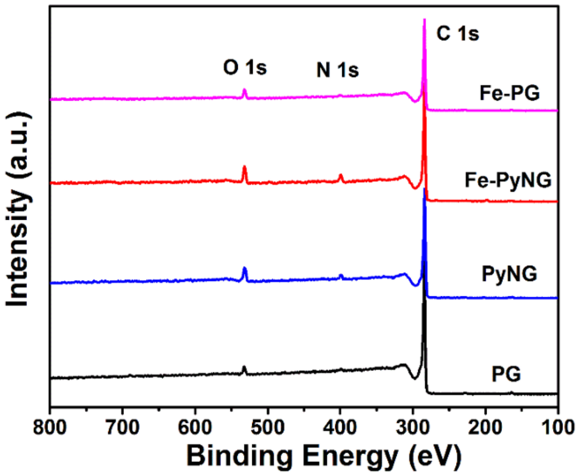

**Figure S2.** XPS survey spectra of PG, PyNG, Fe-PyNG and Fe-PG.

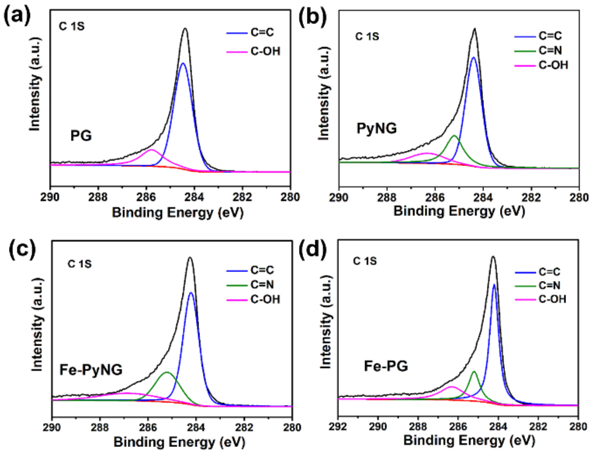

**Figure S3.** C1s XPS spectra of (a) PG, (b) PyNG, (c) Fe-PyNG and (d) Fe-PG.

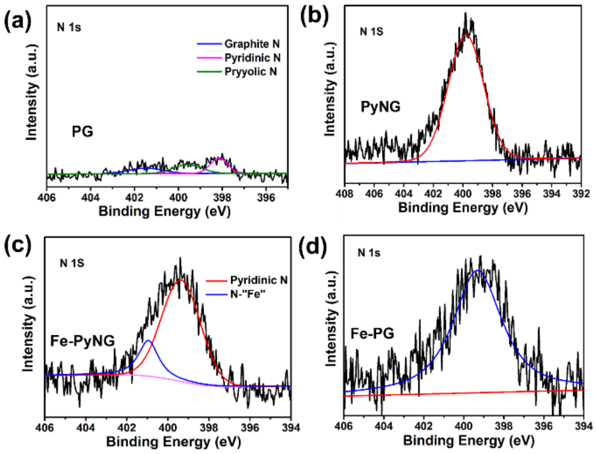

**Figure S4**. N1s XPS spectra of (a) PG and (b) PyNG, (c) Fe-PyNG and (d) Fe-PG.

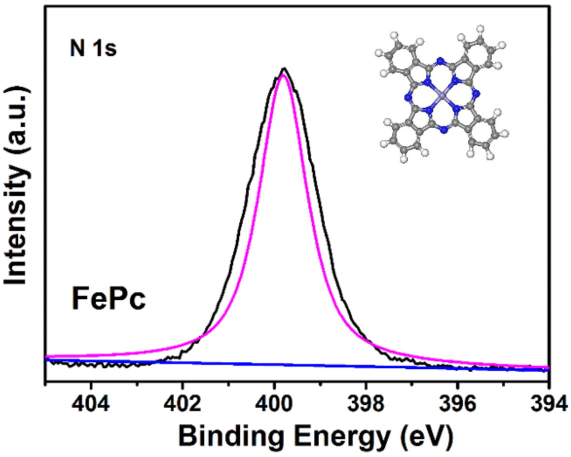

**Figure S5.** N1s XPS spectra of FePc.

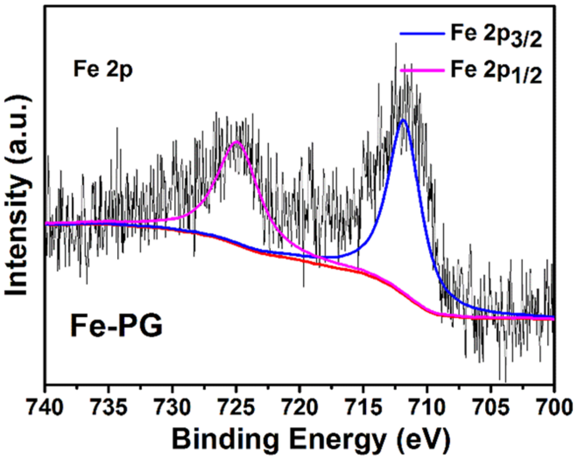

**Figure S6.** Fe2p XPS spectra of Fe-PG.

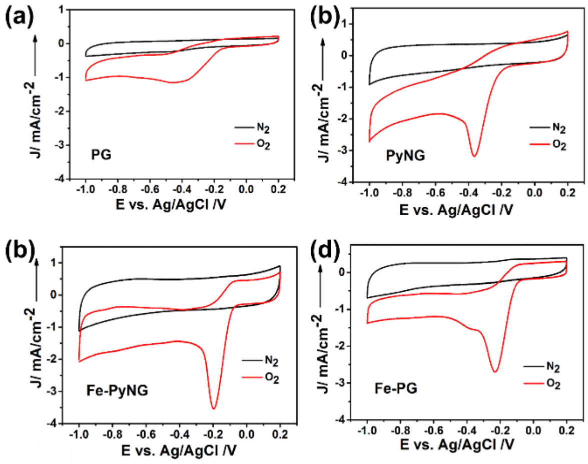

**Figure S7.** CVs of (a) PG, (b) PyNG, (c) Fe-PyNG and (d) Fe-PG in $N_2$ and $O_2$ saturated 0.1 M KOH.

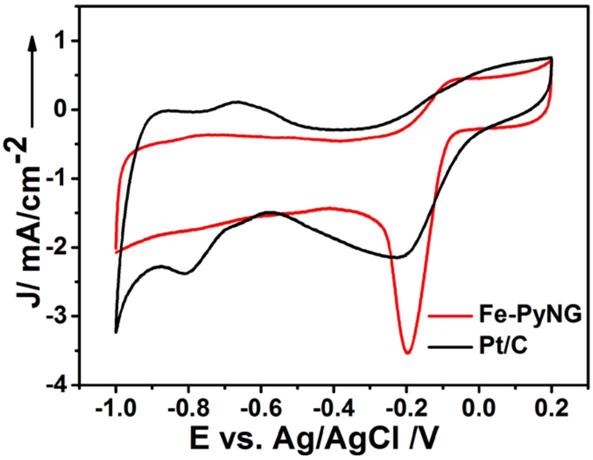

**Figure S8.** Comparison CVs of commercial Pt/C and Fe-PyNG in $O_2$-saturated 0.1 M KOH.

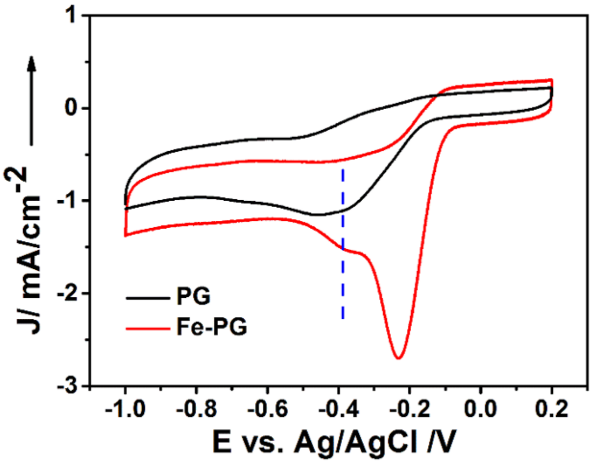

**Figure S9.** Comparison CVs of PG and Fe-PG in $O_2$-saturated 0.1 M KOH.

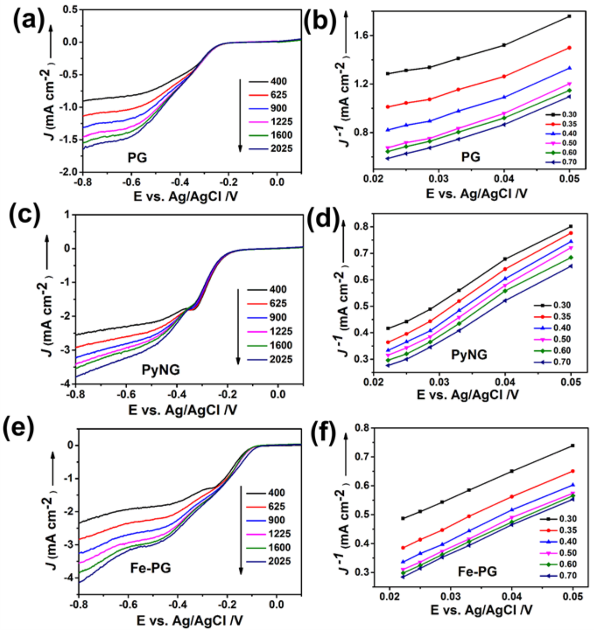

**Figure S10.** LSV of (a) PG, (c) PyNG and (e) Fe-PG on RDE at different rotating rates (400 to 2,025 rpm). Corresponding Koutecky–Levich plot of (b) PG, (d) PyNG and (f) Fe-PG at different potentials.

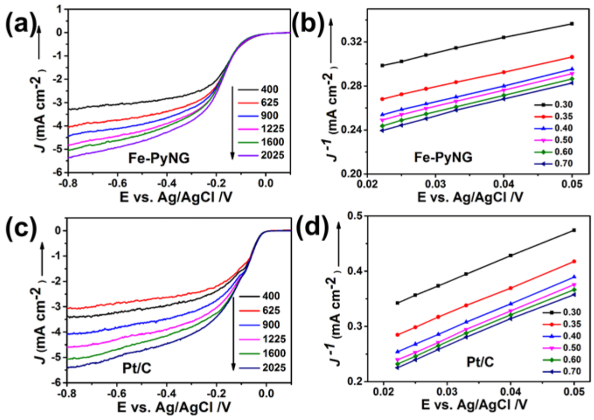

**Figure S11.** LSV of (a) Fe-PyNG, (c) Pt/C on RDE at different rotating rates (400 to 2,025 rpm). Corresponding Koutecky–Levich plot of (b) Fe-PyNG, (d) Pt/C at different potentials.

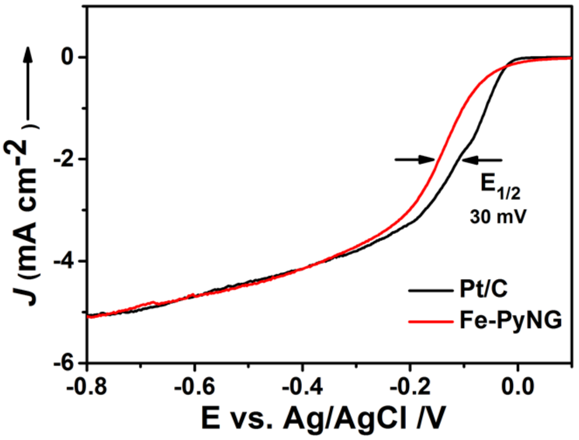

**Figure S12.** LSV of Fe-PyNG and commercial Pt/C catalyst.

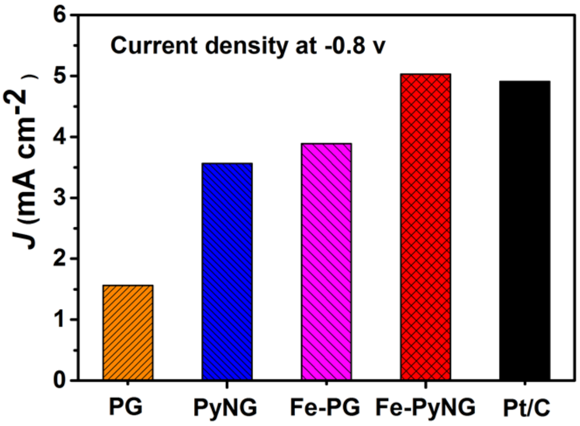

**Figure S13.** Current density of PG, PyNG, Fe-PyNG and Fe-PG at -0.8 V

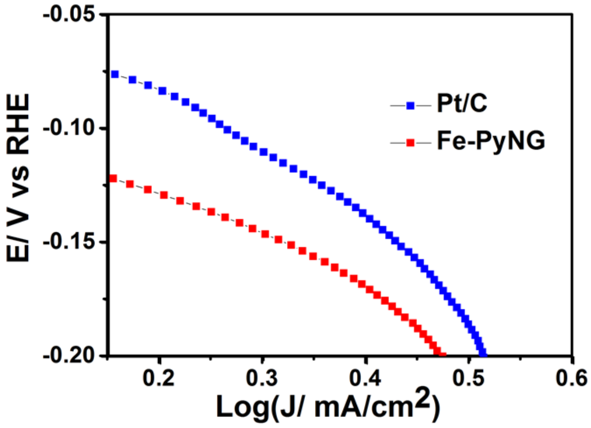

**Figure S14.** Tafel plots for Fe-PyNG and Pt/C extracted from Fig. S11.

# 3. Computational Calculation Section

## 3.1 Models and Method

All of calculations were performed using the Vienna ab initio simulation package (VASP),[2-4] a periodic density functional theory (DFT) code with projector augmented wave (PAW) potentials. The including vdw interactions in

VASP code was implemented via a self-consistent vdw-DFT functional.[5, 6] In this study, the vdw-DF functional with PBE exchange were used, which can well describe the weak interactions, for example van der Waals. The molecues or clusters (OOH, FePc, OOH/FePc) putted in a 20×20×20 Å unit cell were fully relaxed. For Fe-PG, Fe-PyNG and OOH adsorption on these models, the periodic unit cell was used. The Brillouin zone integration was performed using the Monkhorst-Pack scheme with 6×6×1 periodic models and the gamma points were used for clusters. All structures were optimized with a convergence criterion of 10 meV/ Å for the forces and 0.01 meV for the energy. The adsorption energies of molecules on substrates (surfaces or clusters) were defined as $E_{ad}=E_{total}-E_{mol}-E_{sub}$, where $E_{total}$, $E_{mol}$ and $E_{sub}$ are total energies of the adsorbed system, the isolated molecule, and the clean substrate system, respectively.

### 3.2 Computational Calculation results

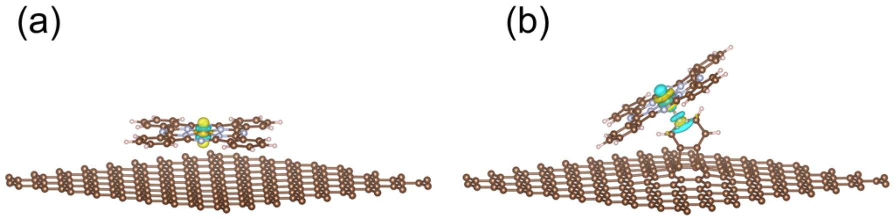

**Figure S15.** Induced charge rearrangements upon adsorption of FePc on PG, and PyNG. Blue (yellow) isosurfaces indicate depletion (addition) of 0.036 $e^{-}/Å^{3}$

## 4. References

1. F. I. Carroll, T. P. Robinson, L. E. Brieaddy, R. N. Atkinson, S. W. Mascarella, M. I. Damaj, B. R. Martin and H. A. Navarro, *J. Med. Chem.*, 2007, **50**, 6383-6391.
2. G. Kresse and J. Hafner, *Phys Rev B*, 1993, **48**, 13115-13118.
3. G. Kresse and J. Furthmuller, *Phys Rev B*, 1996, **54**, 11169-11186.
4. G. Kresse and D. Joubert, *Phys Rev B*, 1999, **59**, 1758-1775.
5. M. Dion, H. Rydberg, E. Schroder, D. C. Langreth and B. I. Lundqvist, *Phys Rev Lett*, 2004, **92**, 246401.
6. A. Gulans, M. J. Puska and R. M. Nieminen, *Phys Rev B*, 2009, **79**, 201105.